

Polymer-grafted and neat vanadium(V) complexes as functional mimics of haloperoxidases



Mannar R. Maurya^{a,*}, Nikita Chaudhary^a, Fernando Avecilla^b

^a Department of Chemistry, Indian Institute of Technology Roorkee, Roorkee 247 667, India

^b Departamento de Química Fundamental, Universidade da Coruña, Campus de A Zapateira, 15071 A Coruña, Spain

ARTICLE INFO

Article history:

Received 22 June 2013

Accepted 15 September 2013

Available online 8 October 2013

Keywords:

Vanadium complexes

Polymer-grafted vanadium complex

Crystal structure

Oxidative bromination of styrene

Oxidative bromination of salicylaldehyde

Oxidative bromination of *trans*-stilbene

ABSTRACT

The monobasic tridentate ONN donor ligand 1-(2-pyridylazo)-2-naphthol [Hpan (**1**)] reacts with $[V^{IV}O(acac)_2]$ in dry methanol to yield the oxidovanadium(IV) complex $[V^{IV}O(acac)(pan)]$ (**1**). The dioxidovanadium(V) complex $[(V^{V}O(pan))_2(\mu-O)_2]$ (**2**) is obtained by aerial oxidation of **1** in methanol. Complex **2** can also be prepared directly by reacting $[V^{IV}O(acac)_2]$ with **1** followed by aerial oxidation in methanol. Treatment of **1** or **2** in methanol with H_2O_2 yields the oxidomonoperoxidovanadium(V) complex $[V^{V}O(O_2)(pan)(MeOH)]$ (**3**). Reaction of imidazolomethylpolystyrene cross-linked with 5% divinylbenzene (PS-im) with **2** in DMF resulted in the formation of the polymer-grafted dioxidovanadium(V) complex PS-im $[V^{V}O_2(pan)]$ (**4**). All these complexes are characterized by various spectroscopic techniques (IR, electronic, NMR (1H and ^{51}V) and electron paramagnetic resonance (EPR)), thermal, field-emission scanning electron micrographs (FE-SEM) as well as energy dispersive X-ray (EDX) studies. The crystal and molecular structure of **3** has been determined, confirming the ONN binding mode of **1**. The polymer-grafted complex **4** has been used for the oxidative bromination of styrene, salicylaldehyde and *trans*-stilbene. Various parameters, such as amounts of catalyst, oxidant (aqueous 30% H_2O_2), KBr and aqueous 70% $HClO_4$ have been optimized to obtain the maximum oxidative bromination of the substrates. Under the optimized reaction conditions, styrene gave a maximum of 99% conversion after 2 h of reaction, with the main products having a selectivity order of: 1-phenylethane-1,2-diol (75%) > 2-bromo-1-phenylethane-1-ol (20%) > 1,2-dibromo-1-phenylethane (1.2%). With nearly same conversion in same time, the oxidative bromination of salicylaldehyde gave three products with the selectivity order: 5-bromosalicylaldehyde > 2,4,6-tribromophenol > 3,5-dibromosalicylaldehyde. A maximum of 91% conversion of *trans*-stilbene has been obtained in 2 h of reaction time, where selectivity of the obtained reaction products varied in the order: 2,3-diphenyloxirane (*trans*-stilbene oxide) > 1,2-dibromo-1,2-diphenylethane > 2-bromo-1,2-diphenylethanol. The catalytic activity of the non-polymer grafted complex **2** is lower than that of the polymer-grafted one. In addition, the recycling ability of the grafted complex makes it better over the neat complex.

© 2013 Elsevier Ltd. All rights reserved.

1. Introduction

The trigonal–bipyramidal coordination environment of the vanadium center in vanadate-dependent haloperoxidases (VHPO) enzymes, irrespective of their origin [1–4], has stimulated the coordination chemistry of vanadium, with particular emphasis on the model character of vanadium(V) complexes having O and N functionalities. These structural models have also been extended to functional similarities including other catalytic potentials in oxygen transformations [5–11]. $V^{V}O_2$ complexes with tridentate (ONO or ONN) ligand systems provide mostly a five-coordinate environment to the vanadium center, similar to the enzymes.

However, such complexes are coordinatively unsaturated and have a tendency to attain a six coordination environment [12]. This is mostly achieved through the coordination of a solvent molecule, if a suitable functional group of a neighboring molecule for the formation of bridging complex is not available [13–15]. The replacement of a coordinated solvent molecule in such model complexes by an imidazole moiety, one of the binding sites in VHPO, pre-grafted in a polymer produces immobilized structural models that can be modified to functional models for continuous working without losing their catalytic activities [8,16,17].

Herein, we have prepared the dioxidovanadium(V) complex of a tridentate ONN donor ligand, 1-(2-pyridylazo)-2-naphthol [Hpan (**1**)], and have grafted the complex through coordination of an imidazole functionalized chloromethylated polystyrene (cross-linked with 5% divinylbenzene). The characterization of the immobilized

* Corresponding author. Tel.: +91 1332 285327; fax: +91 1332 273560.

E-mail address: rkmanfyc@iitr.ac.in (M.R. Maurya).

as well as neat complexes, their reactivity and catalytic potential as functional mimics for the oxidative bromination of organic substrates have been reported.

2. Experimental

2.1. Materials

V₂O₅ (Loba Chemie, Mumbai, India), acetylacetone (Hacac), 1-(2-pyridylazo)-2-naphthol (Aldrich Chemicals Co., USA), salicylaldehyde (Sisco research, India), styrene (Acros Organics, USA), *trans*-stilbene (Lancaster, England) and aqueous 30% H₂O₂ (Qualigens, India) were used as obtained. Chloromethylated polystyrene [18.9% Cl (5.35 mmol Cl per gram of resin)] cross-linked with 5% divinylbenzene was obtained as a gift from Thermax Limited, Pune, India. [V^{IV}O(acac)₂] was prepared according to the methods reported [18].

2.2. Physical methods and analysis

Elemental analyses of the ligand and complexes were obtained with an Elementar model Vario-EL-III. The vanadium content in the polymer-grafted complex was checked by Inductively Coupled Plasma spectrometry (ICP; Labtam 8440 plasma lab). Thermogravimetric analyses of the complexes were carried out using a Perkin-Elmer Pyris Diamond under an oxygen atmosphere. The energy dispersive X-ray analyses (EDX) of the anchored ligand and the complex were recorded on an FEI Quanta 200 FEG. The samples were coated with a thin film of gold dust to protect the surface material from thermal damage by the electron beam and to make the sample conductive. IR spectra were recorded as KBr pellets on a Nicolet NEXUS Aligent 1100 FT-IR spectrometer after grinding the sample with KBr. The electronic spectrum of a solid sample was recorded in Nujol using a Shimadzu 1601 UV-Vis spectrophotometer by layering the mull of the sample to the inside of one of the cuvettes while keeping the other one layered with Nujol as a reference. Spectra of neat complexes were recorded in methanol or DMSO. ¹H and ⁵¹V NMR spectra were obtained on Bruker Avance III 500 and 400 MHz spectrometers, respectively, with the common parameter settings. NMR spectra were usually recorded in MeOD-*d*₄ or DMSO-*d*₆, and δ(⁵¹V) values are referenced relative to neat VOCl₃ as an external standard. The EPR spectrum was recorded with a Bruker EMX EPR X-band spectrometer. The spin Hamiltonian parameters were obtained by simulation of the spectrum with the computer program of Rockenbauer and Korecz [19]. A Shimadzu 2010 plus gas-chromatograph fitted with a Rtx-1 capillary column (30 m × 0.25 mm × 0.25 μm) and an FID detector was used to analyze the reaction products. The percent conversion of substrate and the selectivity of the products were made on the basis of the relative peak area of the substrate/respective product in the GC using a formulae presented elsewhere [20]. The identity of the products was confirmed using a GC-MS model Perkin-Elmer, Clarus 500 by comparing the fragments of each product with the library available.

2.3. Preparations

2.3.1. Preparation of [V^{IV}O(acac)₂](pan)] (1)

A stirred solution of [V^{IV}O(acac)₂] (0.53 g, 2 mmol) dissolved in methanol (20 mL) was added to a hot solution of Hpan (0.498 g, 2 mmol) in methanol (25 mL) and the resulting reaction mixture was refluxed for ca. 8 h in an oil bath. The obtained dark brown precipitate was filtered off, washed with methanol and dried in a vacuum. Yield 72%. *Anal. Calc.* for C₂₀H₁₇N₃O₄V (414.31): C, 57.98; H, 4.14; N, 10.14. Found: C, 57.5; H, 4.0; N, 10.2%.

2.3.2. [{V^{VO}(pan)]₂(μ-O)₂] (2)

Complex **1** (0.414 g, 1 mmol) was dissolved in hot methanol (100 mL) and air was passed through the solution with stirring and occasional heating. After ca. 3 days the solution slowly changed to a wine red colour. After reducing the volume and keeping the solution at room temperature, complex **2** slowly precipitated, which was filtered and dried at ca. 100 °C. Yield 85%. *Anal. Calc.* for C₃₀H₂₀N₆O₆V₂ (662.41): C, 54.40; H, 3.04; N, 12.69. Found: C, 53.8; H, 2.9; N, 12.5%. ¹H NMR (DMSO-*d*₆/δ in ppm): 7.15–7.17 (d, 1H), 7.49–7.52 (t, 1H), 7.72–7.75 (q, br, 2H), 7.90–7.92 (d, 1H), 8.12–8.14 (d, 1H), 8.26–8.28 (d, 1H), 8.38–8.41 (t, 1H), 9.33–9.34 (d, 1H), 9.36–9.37 (d, 1H). ⁵¹V NMR (MeOD-*d*₄/δ in ppm): –542 (major and sharp), –549 (minor).

2.3.3. [V^{VO}(O₂)(pan)(MeOH)] (3)

Aqueous 30% H₂O₂ (ca. 2 mL) was added dropwise to complex **1** (0.414 g, 1 mmol) suspended in methanol (30 mL) with constant stirring at ambient temperature. After ca. 8 h, the insoluble complex slowly dissolved and gave a pinkish red solution. The solution was kept for ca. 24 h after reducing the solution volume to ca. 10 mL. The precipitated solid was filtered, washed with cold methanol (2 × 4 mL) and dried in air. Yield 50%. *Anal. Calc.* for C₁₆H₁₄N₃O₅V (379.25): C, 50.67; H, 3.72; N, 11.07. Found: C, 51.1; H, 3.8; N, 11.2%. IR (KBr, ν_{max}, cm⁻¹): 1359 (N=N_{azo}), 935 (V=O), 848 (O–O), 771 [V(O)₂ *asym*], 562 [V(O)₂ *sym*]. ¹H NMR (DMSO-*d*₆/δ in ppm): 3.16–3.17 (d, 3H), 4.07–4.10 (q, 1H), 6.65–6.67 (d, 1H), 7.24–7.31 (t, br, 1H), 7.56–7.59 (t, 1H), 7.67–7.69 (d, 1H), 7.90–7.92 (d, 1H), 7.99 (s, 2H), 8.38–8.92 (t, 2H). ⁵¹V NMR (MeOD-*d*₄/δ in ppm): –597.

2.3.4. Preparation of PS-im[V^{VO}O₂(pan)] (4)

Imidazolomethylpolystyrene (PS-im) [16] (1.00 g) was allowed to swell in DMF (20 mL) for 2 h. A solution of [{V^{VO}(pan)]₂(μ-O)₂] (**2**) (1 g, 3.02 mmol) in DMF (20 mL) was added to the above suspension and the reaction mixture was heated at 90 °C for 14 h with slow mechanical stirring. After cooling to room temperature, the dark black polymer-grafted complex **4** was separated by filtration, washed with hot DMF, followed by hot methanol and dried at 120 °C in an air oven. Found: V, 1.12%.

2.4. X-ray crystal structure determination

Three-dimensional room temperature X-ray data for **3** were collected on a Bruker Kappa Apex CCD diffractometer at low temperature by the φ-ω scan method. Reflections were measured from a hemisphere of data collected from frames, each of them covering 0.3° in ω. Of the 15840 reflections measured for **3**, all were corrected for Lorentz and polarization effects and for absorption by multi-scan methods based on symmetry-equivalent and repeated reflections, 1575 independent reflections exceeded the significance level ($|F|/σ|F|$) > 4.0. Complex scattering factors were taken from the program package SHELXTL [21]. The structure was solved by the direct method and refined by full matrix least-squares on F². Hydrogen atoms were located in the difference Fourier map and freely refined, except for the hydrogen atoms of C(7) and O(1M), which were included in calculation positions and refined in the riding mode. Refinement was done with allowance for thermal anisotropy of all non-hydrogen atoms. Further details of the crystal structure determination are given in Table 1. A final difference Fourier map showed no residual density outside: 0.628 and –0.852 e Å⁻³. A weighting scheme, $w = 1/[σ^2(F_o^2) + (0.057800 - P)^2 + 0.602000P]$, where $P = (|F_o|^2 + 2|F_c|^2)/3$, was used in the later stages of the refinement.

Table 1
Crystal data and structure refinement for **3**.

Compound	3
Formula	C ₁₆ H ₁₄ N ₃ O ₅ V
Formula weight	379.24
T (K)	100(2)
λ (Å)	0.71073
Crystal system	monoclinic
Space group	P2 ₁ /c
a (Å)	8.827(7)
b (Å)	9.970(7)
c (Å)	17.633(14)
β (°)	91.39(2)
V (Å ³)	1551(2)
Z	4
F (000)	776
D _{calc} (g cm ⁻³)	1.624
μ (mm ⁻¹)	0.674
θ (°)	2.31–27.69
R _{int}	0.2179
Crystal size (mm ³)	0.20 × 0.14 × 0.05
Goodness-of-fit (GOF) on F ²	1.007
R ₁ ^a	0.0819
wR ₂ (all data) ^b	0.1874
Largest differences peak and hole (e Å ⁻³)	0.647 and –0.876

^a $R_1 = \sum ||F_o| - |F_c|| / \sum |F_o|$.

^b $wR_2 = \{ \sum [w(|F_o|^2 - |F_c|^2)]^2 / \sum [w(F_o^4)] \}^{1/2}$.

2.5. Catalytic activity studies

Warning: HClO₄ is potential oxidant, hence must be handled carefully.

The polymer-grafted complex PS-im[V^{VO}₂(pan)] (**4**) was used for the oxidative bromination of styrene, salicylaldehyde and *trans*-stilbene. All reactions were carried out in a 50 mL round bottom flask at 40 °C. The polymer beads were allowed to swell in methanol for 2 h prior to the start of the catalytic reaction.

2.5.1. Oxidative bromination of styrene

The catalyst (0.010 g), styrene (1.04 g, 10 mmol), KBr (2.38 g, 20 mmol), aqueous 30% H₂O₂ (2.27 g, 20 mmol) and 70% aqueous HClO₄ (5.72 g, 40 mmol, added in four equal portions at $t = 0, 15, 30$ and 45 min) were stirred at 40 °C in a two phase CH₂Cl₂–H₂O (40 mL 50%, v/v mixture) system for 1 h. Every 15 min a small aliquot was withdrawn and after addition of 5 mL of CH₂Cl₂, it was washed with distilled water in a separating funnel and the organic layer was analyzed by gas chromatography. At the end of the reaction, the organic layer after processing as above, was evaporated and the residue was purified by column chromatography using 1% CH₂Cl₂ in *n*-hexane as an eluent. The products were identified by GC–MS and ¹H NMR spectroscopy.

1,2-Dibromo-1-phenylethane: ¹H NMR (CDCl₃/δ in ppm): 7.29–7.39 (m, 5H, aromatic), 5.11–5.13 (q, 1 H, CH), 3.97–4.06 (septet, 2H, CH₂).

1-Phenylethane-1,2-diol: ¹H NMR (CDCl₃/δ in ppm): 7.29–7.39 (m, 5H, aromatic), 4.9 (q, 1H, CH), 3.5 (q, 1H of CH₂), 3.6 (q, 1H of CH₂), 2.7 (br, 1H, OH).

2-Bromo-1-phenylethane-1-ol: ¹H NMR (CDCl₃/δ in ppm): 7.29–7.39 (m, 5H, aromatic), 5.1 (q, 1H, CH), 3.9 (septet, 2H, CH₂).

These data matched well with those reported earlier [22].

2.5.2. Oxidative bromination of salicylaldehyde

The catalyst (0.005 g), salicylaldehyde (0.61 g, 5 mmol), KBr (1.18 g, 10 mmol), 30% H₂O₂ (1.13 g, 10 mmol) and 70% HClO₄ (1.42 g, 10 mmol, added in four equal portions at $t = 0, 30, 60$ and 90 min) were stirred at 40 °C in distilled water (20 mL) for 2 h. After completion of the reaction, it was transferred to a separating funnel and washed several times with water after addition of 10 mL of

CH₂Cl₂. The organic layer was analyzed by gas chromatography and the reaction products were identified by GC–MS analysis.

2.5.3. Oxidative bromination of *trans*-stilbene

The catalyst (0.005 g), *trans*-stilbene (0.90 g, 5 mmol), KBr (3.56 g, 30 mmol), 30% H₂O₂ (3.39 g, 30 mmol) and 70% HClO₄ (5.72 g, 40 mmol) (added in four equal portions as mentioned before) were taken in a two phase CHCl₃–H₂O (40 mL, 50%, v/v) mixture system and stirred at 40 °C. After 2 h the reaction mixture was washed with water and the organic layer was separated. The obtained reaction products were analyzed as mentioned above using this organic layer. For the identification of the reaction products the crude mass was suspended in CH₂Cl₂; the insoluble *trans*-stilbene oxide was separated by filtration, and then the solvent was evaporated. Other reaction products were separated using a silica gel column. Elution of the column with 1% CH₂Cl₂ in *n*-hexane first separated the mono bromo derivative, followed by the dibromo derivative. The products were identified by GC–MS and ¹H NMR spectroscopy.

¹H NMR spectral data of reaction products are as follows:

2,3-Diphenyloxirane: ¹H NMR (CDCl₃/δ in ppm): 7.35–7.55 (m, 10H, aromatic); 5.5 (d, 2H, CH).

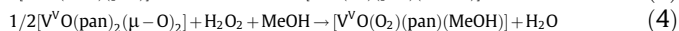
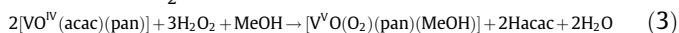
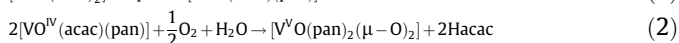
2-Bromo-1,2-diphenylethanol: ¹H NMR (CDCl₃/δ in ppm): 8.0 (s, 1H, OH); 7.37–7.52 (m, 10H, aromatic); 5.5 (d, 2H, CH).

1,2-Dibromo-1,2-diphenylethane: ¹H NMR (CDCl₃/δ in ppm): 7.1–7.4 (m, 10H, aromatic); 6.15 (d, 2H, CH).

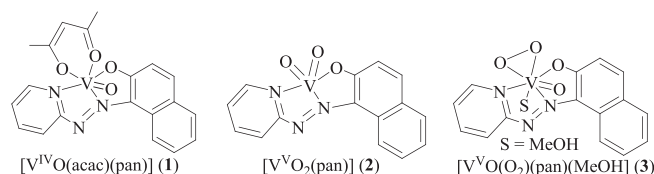
3. Results and discussion

3.1. Synthesis, characterization and solid state characteristics

The reaction between equimolar amounts of [V^{IV}O(acac)₂] and Hpan (**1**) in dry, refluxing methanol yielded the oxidovanadium(IV) complex [V^{VO}O(acac)(pan)] (**1**) (Eq. (1)). On aerial oxidation of **1** in methanol, the dioxidovanadium(V) complex {[V^{VO}O(pan)]₂(μ-O)₂} (**2**) was obtained (Eq. (2)). Complex **2** can also be prepared directly by reacting [V^{IV}O(acac)₂] with **1** followed by aerial oxidation. Addition of H₂O₂ to a methanolic solution of **1** yielded the oxidomonoperoxidovanadium(V) complex [V^{VO}O(O₂)(pan)(MeOH)] (**3**) (Eq. (3)). Same complex could also be isolated by the reaction of **2** with H₂O₂ in methanol (Eq. (4)).



All the complexes are fairly soluble in methanol, CHCl₃, DMF and DMSO; complex **1** is additionally soluble in CH₂Cl₂. Scheme 1 presents the structures proposed for these complexes, which are based on the spectroscopic characterization (IR, electronic, EPR, ¹H and ⁵¹V NMR), elemental analyses, thermogravimetric patterns and single crystal X-ray analysis of **3**. The ligand coordinates through its monoanionic (ONN) functionalities.



Scheme 1. Proposed structures of the complexes prepared. Only the idealized structure of **2** is shown.

Immobilization of imidazole through covalent attachment onto chloromethylated polystyrene, cross-linked with 5% divinylbenzene (imidazolomethylpolystyrene, PS-im) has been achieved in acetonitrile in the presence of KI and triethylamine, following the literature procedure (Scheme 2) [16,17]. The remaining chlorine content of 0.166 mmol/g in imidazolomethylpolystyrene (PS-im) suggests ca. 97% substitution of imidazole. Reaction of PS-im with complex **2** in DMF resulted in the formation of the polymer-grafted dioxido vanadium(V) complex PS-im[V^VO₂(pan)] (**4**). The free chloromethyl groups of PS do not coordinate with the vanadium precursor. Scheme 2 presents the whole synthetic procedure. The metal ion loading calculated from the obtained vanadium content (0.21 mmol/g of resin) for PS-im[VO₂(pan)] is also close to the value determined by thermogravimetric analysis (0.18 mmol/g of resin).

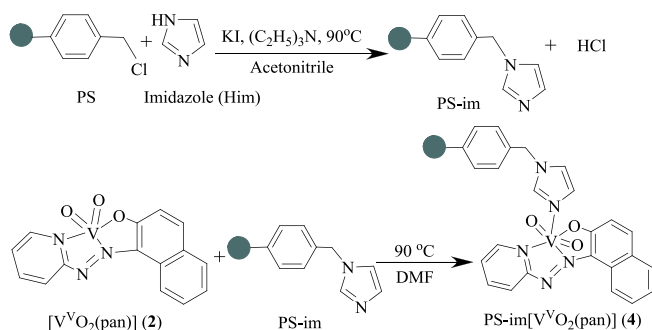
3.2. Structure description of [V^VO(O₂)(pan)(MeOH)] (**3**)

The complex [V^VO(O₂)(pan)(MeOH)] (**3**) crystallizes from methanol as dark red prisms (crystal dimensions 0.22 × 0.21 × 0.20). Fig. 1 shows an ORTEP representation of **3** and Table 2 contains selected bond lengths and angles. The vanadium atom is in the oxidation state V. In the molecular structure, the vanadium center adopts a distorted seven-coordinated pentagonal bipyramidal geometry with the (pan) ligand coordinated through one O_{naphthol}, one N_{azo} and one N_{pyridine} atom, and with one O_{oxide} (terminal), one O_{methanol} and two O_{peroxide}, O(2) and O(3), atoms also coordinated to the vanadium centre. The peroxide O–O distance of 1.443(5) Å lies within the range (1.38–1.45 Å) of the majority of peroxide compounds [23–25]; the distances V(1)–O(2) of 1.889(4) Å and V(1)–O(3) of 1.856(4) Å also indicate the presence of a peroxide group.

The V=O bond [V(1)–O(4): 1.600(4) Å] is characteristic of an oxido-type O atom with strong π bonding (see Table 2). The V–O_{methanol} bond, which is trans to the oxo atom, is significantly longer [V(1)–O(1M): 2.241(4) Å] [11]. Intermolecular hydrogen bonds occur between the bonded methanol group and the two oxygen atoms of the peroxide group of another molecule (see Fig. 2 and Table 3). The pan ligand has a planar structure in the complex. The vanadium atom is displaced by about 0.2743 Å from the plane constituted for all the atoms of the ligand [C(1), C(2), C(3), C(4), C(5), C(6), C(7), C(8), C(9), C(10), C(11), C(12), C(13), C(14), C(15), N(1), N(2) and N(3)], which presents a deviation from planarity of 0.0498(56) Å.

3.3. Thermogravimetric analysis (TGA) studies

The complex [VO^{IV}(acac)(pan)] (**1**) decomposes exothermally in two major steps. Between 200 and 480 °C, the weight loss corresponds to removal of the acac ligand (Found: 23.6, Calc.: 23.9%). On



Scheme 2. Synthetic procedure for the isolation of the polymer-grafted dioxido vanadium(V) complex, PS-im[VO₂(pan)] (**4**). The ball represents the polystyrene back-bone.

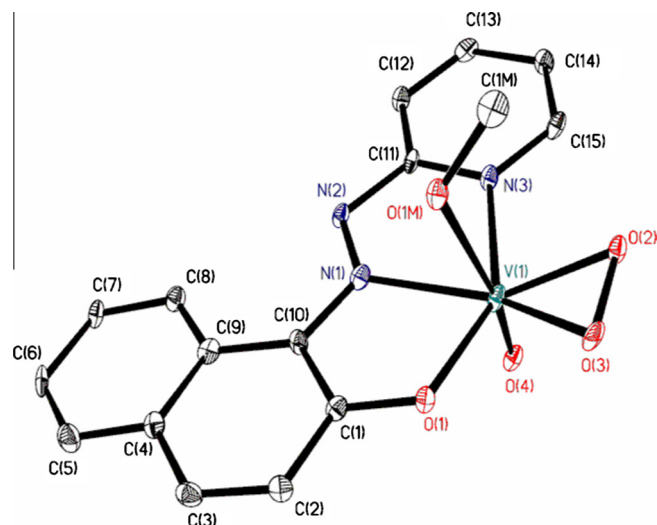


Fig. 1. ORTEP plot of the complex [V^VO(O₂)(pan)(MeOH)] (**3**). All non-hydrogen atoms are presented by their 30% probability ellipsoids. Hydrogen atoms are omitted for clarity.

Table 2
Bond lengths (Å) and angles (°) for [V^VO(O₂)(pan)(MeOH)] (**3**).

3			
<i>Bond lengths (Å)</i>			
V(1)–O(1)	2.000(4)	O(2)–O(3)	1.443(5)
V(1)–O(2)	1.889(4)	V(1)–N(1)	2.135(5)
V(1)–O(3)	1.856(4)	V(1)–N(3)	2.115(5)
V(1)–O(4)	1.600(4)	N(1)–N(2)	1.275(6)
V(1)–O(1M)	2.241(4)		
<i>Bond Angles (°)</i>			
O(4)–V(1)–O(3)	105.5(2)	O(3)–V(1)–N(1)	152.30(19)
O(4)–V(1)–O(2)	104.1(2)	O(2)–V(1)–N(1)	151.2(2)
O(3)–V(1)–O(2)	45.30(17)	O(1)–V(1)–N(1)	75.91(19)
O(4)–V(1)–O(1)	97.7(2)	N(3)–V(1)–N(1)	72.3(2)
O(3)–V(1)–O(1)	80.05(17)	O(4)–V(1)–O(1M)	166.82(19)
O(2)–V(1)–O(1)	124.62(18)	O(3)–V(1)–O(1M)	87.52(17)
O(4)–V(1)–N(3)	91.8(2)	O(2)–V(1)–O(1M)	86.32(18)
O(3)–V(1)–N(3)	127.6(2)	O(1)–V(1)–O(1M)	82.47(17)
O(2)–V(1)–N(3)	82.79(19)	N(3)–V(1)–O(1M)	81.34(18)
O(1)–V(1)–N(3)	146.95(18)	N(1)–V(1)–O(1M)	75.95(18)
O(4)–V(1)–N(1)	91.3(2)		

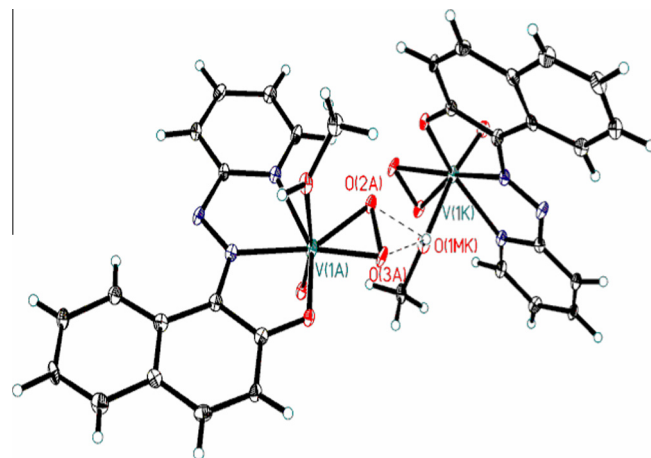


Fig. 2. Hydrogen bonding scheme of the compound [V^VO(O₂)(pan)(MeOH)] (**3**). All the non-hydrogen atoms are presented by their 30% probability ellipsoids.

Table 3
Hydrogen bonds for $[V^{VO}(O_2)(\text{pan})(\text{MeOH})]$ (**3**) (Å and °).

D–H...A	d(D–H)	d(H...A)	d(D...A)	<(DHA)
O(1M)–H(1M)...O(2)#1	0.93	2.05	2.694(6)	125.1
O(1M)–H(1M)...O(3)#1	0.93	2.36	3.157(6)	143.4

Symmetry transformations used to generate equivalent atoms:
#1 $-x + 2, y + 1/2, -z + 1/2$.

further heating the remaining residue decomposes sharply in the range 480–550 °C to give V_2O_5 (Found: 29.0, Calc.: 30.0%) as the end product. The polymer-grafted complex PS-im $[VO_2(\text{pan})]$ (**4**) starts losing weight at ca. 200 °C, but major exothermic decomposition occurs in two overlapping steps in the temperature range 400–500 °C. It was difficult to distinguish the decomposition of the polymer and organic ligand fragments. However, the remaining vanadium content of 0.18 mmol/g of resin suggests the formation of V_2O_5 .

3.4. Field emission-scanning electron microscopic (FE-SEM) and energy dispersive X-ray analysis (EDX) studies

Field emission-scanning electron micrographs (Fe-SEM) for single beads of pure chloromethylated polystyrene and the polymer-grafted complex were recorded to see the morphological changes. Some of these images are reproduced in Fig. 3. As expected, grafting of the vanadium complex resulted in the roughening of the top layer of the polymer-supported beads. Energy dispersive X-ray analyses (EDX) estimate a vanadium content of ca. 0.18 mmol/g of resin for PS-im $[VO_2(\text{pan})]$ (**4**). This observation suggests the immobilization of the metal complex onto the polystyrene beads.

3.5. IR spectral study

Fig. 4 presents the IR spectra of the complexes. The complex $[V^{VO}(\text{acac})(\text{pan})]$ (**1**) shows one sharp band at 955 cm^{-1} in the IR spectrum due to the $\nu(\text{V}=\text{O})$ stretch, while the dioxido complex $[\{V^{VO}(\text{pan})\}_2(\mu\text{-O})_2]$ (**2**) shows one sharp band at 936 cm^{-1} and a broad band at 848 cm^{-1} corresponding to $\nu(\text{V}=\text{O})$ and $\nu(\text{V}=\text{O}\cdots\text{V})$ modes, respectively. This observation hints towards dimerization of complex **2** in the solid state. This dimer breaks into a monomer upon grafting onto the polymer and exhibits $\nu_{\text{asym}}(\text{V}=\text{O})$ and $\nu_{\text{sym}}(\text{O}=\text{V}=\text{O})$ modes at 940 and 917 cm^{-1} , respectively (Table 4). The peroxo complex $[V^{VO}(O_2)(\text{pan})(\text{MeOH})]$ (**3**) exhibits three IR active vibrational modes associated with the peroxido moiety $[V(O_2)]^{2+}$ at 923, 721 and 565 cm^{-1} , which are assigned to the O–O intra stretching, asymmetric $V(O_2)$ stretching and symmetric $V(O_2)$ stretching, respectively. In addition, a band at 960 cm^{-1} is assigned due to the $\nu(\text{V}=\text{O})$ stretch.

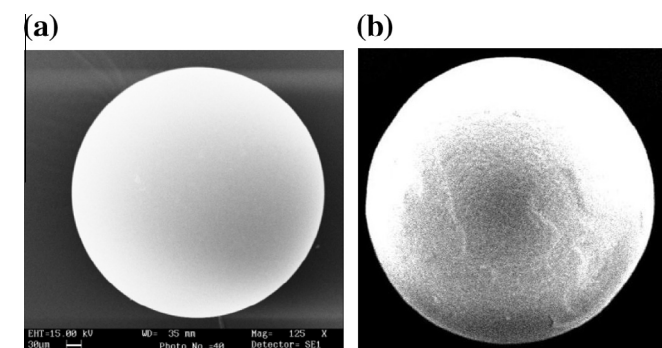


Fig. 3. Field emission-scanning electron micrographs of (a) chloromethylated polystyrene (PS) and (b) PS-im $[VO_2(\text{pan})]$ (**4**).

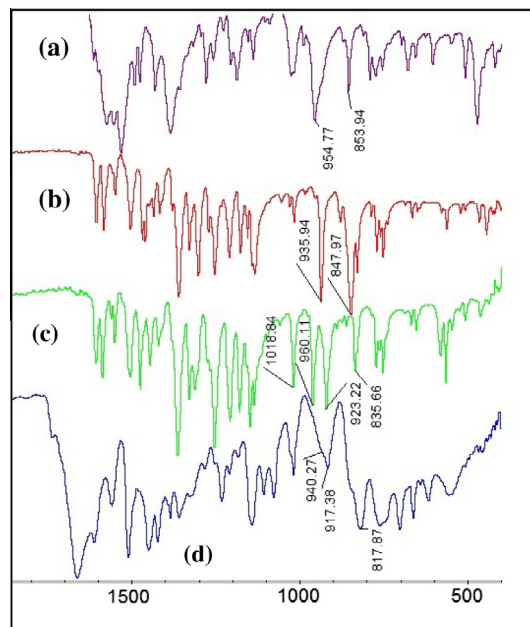


Fig. 4. IR spectra of (a) $[V^{VO}(\text{acac})(\text{pan})]$ (**1**), (b) $[\{V^{VO}(\text{pan})\}_2(\mu\text{-O})_2]$ (**2**), (c) $[V^{VO}(O_2)(\text{pan})(\text{MeOH})]$ (**3**) and (d) PS-im $[VO_2(\text{pan})]$ (**4**).

Table 4
IR spectral data (cm^{-1}) of the ligand and the complexes.

Compounds	$\nu(\text{N}=\text{N}_{\text{azo}})$	$\nu(\text{C}=\text{N}_{\text{pyridyl}}/\text{C}=\text{C})$	$\nu(\text{V}=\text{O})$
Hpan (I)	1436	1566, 1620	–
$[V^{VO}(\text{acac})(\text{pan})]$ (1)	1360	1549, 1586	955
$[\{V^{VO}(\text{pan})\}_2(\mu\text{-O})_2]$ (2)	1359	1550, 1587	936, 848
$[V^{VO}(O_2)(\text{pan})(\text{MeOH})]$ (3) ^a	1359	1550, 1585	960
PS-im $[VO_2(\text{pan})]$ (4)	1364	1560, 1600	940, 917

^a Bands due to the peroxido group: 923, 721 and 565 cm^{-1} .

The IR spectrum of Hpan (**I**) displays a sharp band at 1436 cm^{-1} due to the $\nu(-\text{N}=\text{N}-)$ group. In the complexes, this band shifts to a lower wave number and appears at 1359–1364 cm^{-1} , confirming the coordination of the azo nitrogen to the metal centre [26]. The ligand also exhibits two sharp bands at 1566 and 1620 cm^{-1} due to $\nu(\text{C}=\text{C}/\text{C}=\text{N})$ and both bands appear at lower wavenumbers (1549–1560/1585–1600 cm^{-1}) due to the coordinated ring nitrogen to the metal. The absence of a band in the 3400 cm^{-1} region (in **1**, **2** and **4**) indicates the coordination of the phenolic oxygen after proton replacement. Thus, the IR data confirm the monobasic tridentate ONN coordination behavior of the ligand in these complexes.

3.6. Electronic spectral studies

As the ligand **I** is an azo dye with a phenolic oxygen, complexes of this ligand are highly coloured and show several bands in the visible region. We have recorded the electronic spectra of the complexes in MeOH and DMSO. In general, the complexes $[\{V^{VO}(\text{pan})\}_2(\mu\text{-O})_2]$ (**2**) and $[V^{VO}(O_2)(\text{pan})(\text{MeOH})]$ (**3**) show a good resolution of bands in MeOH, while the complex $[V^{VO}(\text{acac})(\text{pan})]$ (**1**) shows better resolved bands in DMSO. Table 5 provides details of the spectral data in both solvents, but the discussion written below is based on the best spectra obtained for these complexes. The absorption bands appearing at 502, 540 and 567 nm in **1** and at 486, 551 and 580 nm in **2** are due to ligand-to-metal charge transfer type transitions (LMCT). Such bands in **3** appear at 552 and 580 nm. The band appearing at

Table 5
Electronic spectral data of the ligand and the complexes.

Compounds	Solvent	λ_{\max}/nm ($\epsilon/\text{M}^{-1} \text{cm}^{-1}$)
Hpan (1)	MeOH	224, 304, 463
$[\text{V}^{\text{VO}}(\text{acac})(\text{pan})]$ (1)	DMSO	257 (19327), 294 (10113), 340 (5097), 415 (6478), 502 (7425)(sh), 540 (11209), 567 (12414), 745 (85)
	MeOH	225 (20491), 292 (7845), 415 (7790)(sh), 462 (10291), 574 (604)
$[\{\text{V}^{\text{VO}}(\text{pan})\}_2(\mu\text{-O})_2]$ (2)	DMSO	274 (13500)(sh), 309 (8107)(sh), 331 (6290)(sh), 410 (6242), 552 (13107), 573 (13708)
	MeOH	228 (19225), 304 (4886)(sh), 435 (4842)(sh), 486 (4047), 551 (5970), 580 (6259)
$[\text{V}^{\text{VO}}(\text{O}_2)(\text{pan})(\text{MeOH})]$ (3)	DMSO	271 (14491)(sh), 307 (7959)(sh), 326 (7167)(sh), 414 (6946), 550 (169450), 581 (18482)
	MeOH	229 (16286), 269 (7368)(sh), 307 (3498)(sh), 326 (3213)(sh), 421 (3719), 552 (8322), 580 (8973)
PS-im $[\text{V}^{\text{VO}}_2(\text{pan})]$ (4)	Nujol	252, 333, 435, 584, 627

415, 435 and 421 nm in **1**, **2** and **3**, respectively is due to the ligand-to-metal charge-transfer from the phenolate O atom to the d orbitals of vanadium for monomeric dioxidovanadium(V) complexes [27]. Complex **1** also displays a weak shoulder band at 745 nm due to a d-d transition. The higher energy UV region bands, occurring in the range 200–330 nm, are assigned to intra-ligand transitions. The electronic spectrum of polymer-grafted PS-im $[\text{V}^{\text{VO}}_2(\text{pan})]$ (**4**) recorded in Nujol (Fig. 5) exhibits a spectral pattern exactly the same as that of **2**, but with weaker intensities, and thus confirms that the supported complex maintains the same coordination atmosphere as found for the non-grafted one.

3.7. EPR spectroscopy study

Fig. 6 presents the EPR spectrum of a “frozen” (77 K) solution (in MeOH) of $[\text{V}^{\text{VO}}(\text{acac})(\text{pan})]$ (**1**). The hyperfine features and spectrum itself are consistent with binding modes involving (O_{acac} , $\text{O}_{\text{phenolate}}$, N_{imine} , N_{py})_{equatorial} and (O_{acac})_{axial}. Once a particular binding mode is assumed, the value of A_{\parallel} can be estimated using the additivity relationship proposed by Wüthrich [28] and Chasteen [29], with an estimated accuracy of $\pm 3 \times 10^{-4} \text{cm}^{-1}$. However, for the potential donor groups under consideration, their predicted contributions to the parallel hyperfine coupling constant are rather similar ($\text{O}_{\text{acac}} \sim 41.7$, $\text{O}_{\text{phenolate}} \sim 38.9$, $\text{N}_{\text{imine}} \sim 41.6$, $\text{N}_{\text{py}} \sim 40.7$, $\text{O}_{\text{MeOH}} \sim 45.5$, all A_{\parallel} contributions in $\text{cm}^{-1} \times 10^{-4}$) [29,30], hence it is not possible to distinguish between the several plausible binding modes. The spectrum of $[\text{V}^{\text{VO}}(\text{acac})(\text{pan})]$ was simulated [16] and the spin Hamiltonian parameters obtained are g_{\parallel} 1.952, A_{\parallel} $163.5 \times 10^{-4} \text{cm}^{-1}$, A_{\perp} $63.0 \times 10^{-4} \text{cm}^{-1}$ and g_{\perp} 1.981. Thus, the EPR spectrum of $[\text{V}^{\text{VO}}(\text{acac})(\text{pan})]$ in MeOH is in good agreement with an O_2N_2 binding mode. However, the coordination of solvent cannot be ruled out, though this implies the substitution of one of the equatorial donor atoms by an O-atom of the solvent.

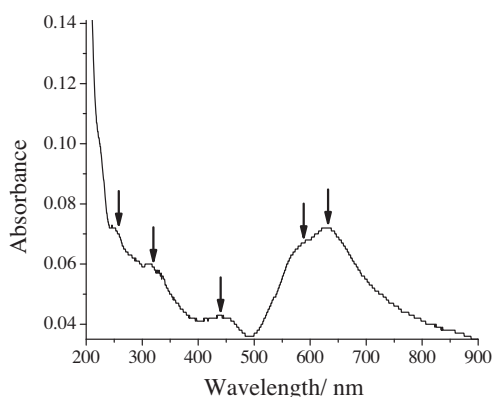


Fig. 5. Electronic spectrum of PS-im $[\text{V}^{\text{VO}}_2(\text{pan})]$ (**4**) recorded after dispersing in Nujol.

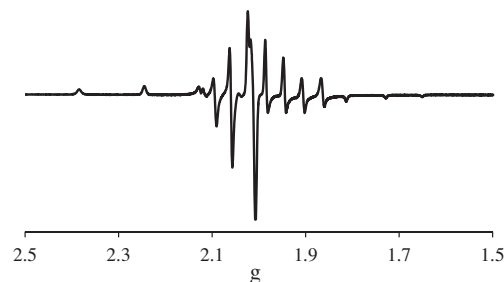


Fig. 6. First derivative EPR spectrum of a frozen solution of $[\text{V}^{\text{VO}}(\text{acac})(\text{pan})]$ (**1**) in MeOH at 77 K.

3.8. ^1H and ^{51}V NMR studies

The ^1H and ^{51}V NMR chemical shift values for the complexes are included in the experimental section. The ^1H NMR spectra of complexes **2** and **3** show all the expected signals. The shielded doublets at 9.33–9.34 (d, 1H) and 9.36–9.37 (d, 1H) ppm in **2** are assignable to the protons nearest to the pyridine-nitrogen and are normally considered as characteristic of a coordinated pyridinic nitrogen [26]. This signal is not very clear in complex **3** as the signals of two protons overlap in this region. Assignments of other aromatic protons are difficult. The ligand Hpan (**1**) displays a signal at $\delta = 15.8$ ppm due the naphtholic proton and the absence of this signal in the complexes confirms the coordination of the naphtholato-O atom.

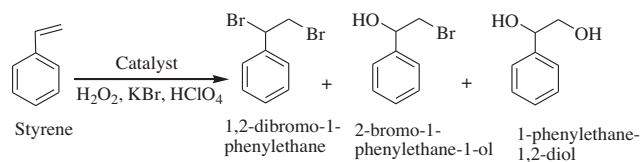
In the ^{51}V NMR spectra, the line widths at half height are typically about 200 Hz. The complex $[\{\text{V}^{\text{VO}}(\text{pan})\}_2(\mu\text{-O})_2]$ (**2**) in MeOD- d_4 displays a sharp resonance at $\delta = -542$ and a minor one at $\delta = -549$ ppm. These chemical shifts are within the values expected for dioxidovanadium(V) complexes containing an O/N donor set [27,31]. The minor signal at $\delta = -549$ ppm gains intensity with time in MeOD- d_4 (24 h), and therefore we assigned this resonance to $[\text{V}^{\text{VO}}_2(\text{pan})(\text{MeOD})]$.

3.9. Catalytic activity studies

Vanadium haloperoxidases catalyze the oxidative bromination of organic substrates in the presence of H_2O_2 and bromide ions; vanadium(V) complexes have been reported to show functional similarities to these enzymes. During the catalytic action vanadium(V) coordinates with 1 or 2 equivalents of H_2O_2 to give oxido-monoperoxido, $[\text{V}^{\text{VO}}(\text{O}_2)]^+$, or oxido-diperoxido, $[\text{VO}(\text{O}_2)_2]^-$, species that oxidize bromide ions in the presence of acid, most likely to Br_2 , Br_3^- and/or HOBr, which ultimately brominate the organic substrates [4,32].

3.9.1. Oxidative bromination of styrene

The dioxidovanadium(V) complexes (polymer grafted as well as non-polymer grafted) reported here satisfactorily catalyze the oxidative bromination of styrene, salicylaldehyde and *trans*-stilbene.



Scheme 3. Oxidative brominated products of styrene.

As also observed earlier [6,22,33], oxidative bromination of styrene in the presence of KBr, HClO_4 and 30% H_2O_2 under a bi-phasic system ($\text{CH}_2\text{Cl}_2\text{-H}_2\text{O}$) gave mainly three major products, 1,2-dibromo-1-phenylethane, 2-bromo-1-phenylethane-1-ol and 1-phenylethane-1,2-diol; **Scheme 3**. Other minor products, like benzaldehyde, styrene epoxide, benzoic acid and 4-bromostyrene, have also been identified, but their overall percentage is extremely low compared to the total of the main products. All major products were separated, identified and confirmed by ^1H NMR spectroscopy as well as GC–MS.

Various reaction parameters, viz. amounts of catalyst, oxidant (30% aqueous H_2O_2), KBr and 70% aqueous HClO_4 , were optimized to obtain the maximum conversion of styrene. For a fixed amount of styrene (1.04 g, 0.010 mol), H_2O_2 (2.27 g, 0.020 mol), KBr (2.38 g, 0.020 mol) and HClO_4 (2.86 g, 0.020 mol, added in four equal portions at $t = 0, 15, 30$ and 45 min of the reaction time) in a $\text{CH}_2\text{Cl}_2\text{-H}_2\text{O}$ (40 mL, v/v) solvent system, three different amounts of catalyst, i.e. 0.010, 0.015 and 0.020 g, were taken and the reaction was carried out at 40 °C for 1 h. As shown in **Fig. 7** (a), a maximum of 65% conversion was achieved with 0.010 g of catalyst. The conversion of styrene improved only marginally to 68% and 70% on increasing the catalyst amount to 0.015 and 0.020 g, respectively. Therefore, 0.010 g amount of catalyst was considered optimum for the maximum conversion of styrene.

Similarly, three different amounts of KBr, i.e. 10, 20 and 30 mmol, were taken for styrene (1.04 g, 10 mmol), catalyst (0.010 g), $\text{CH}_2\text{Cl}_2\text{-H}_2\text{O}$ (40 mL, v/v), 30% aqueous H_2O_2 (2.27 g, 20 mmol) and 70% HClO_4 (2.86 g, 20 mmol, added as mentioned above) and the reaction was carried out at 40 °C. The obtained conversion was comparatively low (41%) with 10 mmol KBr, but increasing the KBr amount from 10 to 20 mmol improved this conversion to 65%, which further improved to 81% at 30 mmol KBr, as shown in **Fig. 7**(b). Therefore, 30 mmol KBr was used to optimize the remaining reaction conditions.

The effect of the amount of oxidant was studied by considering substrate to oxidant ratios of 1:1, 1:2 and 1:3 for a fixed amount of styrene (1.04 g, 10 mmol) under the above reaction conditions. A maximum 64% conversion was achieved with a substrate to oxidant ratio of 1:1. Increasing the substrate to oxidant ratio from 1:1 to 1:2 increased the conversion from 64% to 81%. This conversion further improved considerably (91%) at a substrate to oxidant ratio of 1:3. Only a slight improvement in conversion was obtained upon further increasing this amount. Therefore, an oxidant amount of 30 mmol was considered to be an adequate one [**Fig. 7**(c)] for the maximum conversion of styrene in 1 h of reaction time.

Acid (here HClO_4) was found to be essential to carry out the catalytic bromination. The amount of HClO_4 was optimized by taking substrate to HClO_4 ratios of 1:1, 1:2 and 1:3 under the above reaction conditions; **Fig. 7**(d). For each condition, HClO_4 was added in four equal portion at $t = 0, 15, 30$ and 45 min reaction time. Only 47% conversion was obtained with 10 mmol of HClO_4 (i.e. a 1:1 substrate to HClO_4 ratio), but the conversion reached 91% with 20 mmol of HClO_4 . On increasing this ratio to 1:3, the conversion improved to 98% in 1 h of reaction time. At this ratio, the formation of 1-phenylethane-1,2-diol is relatively more at the expense of 2-bromo-1-phenylethane-1-ol. However, a substrate to HClO_4 ratio

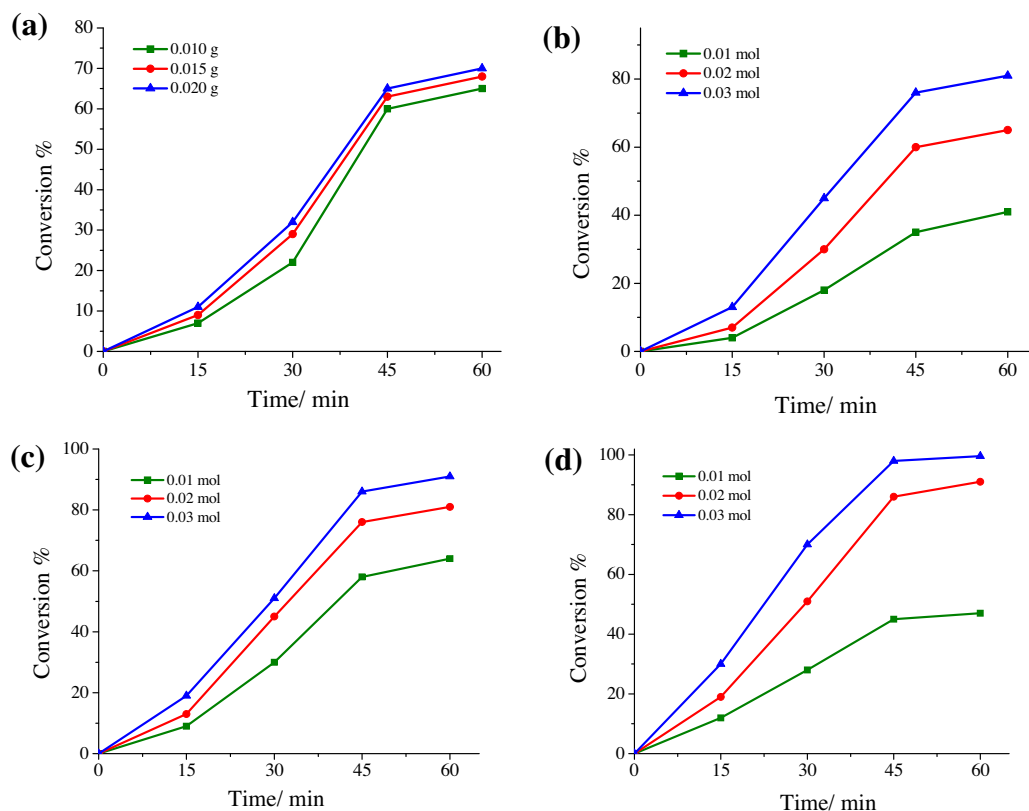
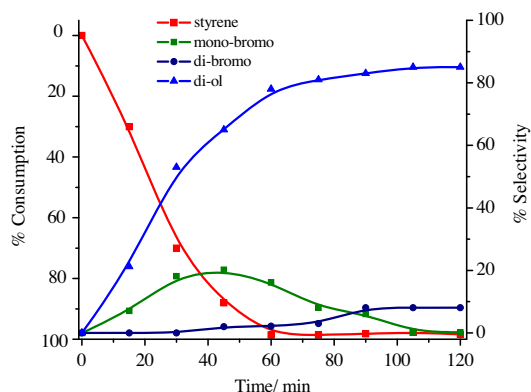


Fig. 7. Effect of (a) amount of catalyst PS-im[VO₂(pan)] (4), (b) amount of KBr, (c) amount of oxidant (i.e. 30% aqueous H_2O_2) and (d) amount of 70% HClO_4 on the oxidative bromination of styrene in 1 h of reaction time. For reaction conditions see text and **Table 6**.

Table 6Results of oxidative bromination of styrene using the catalyst PS-im[VO₂(pan)] after 1 h of reaction time.

Entry No.	KBr (g, mmol)	H ₂ O ₂ (g, mmol)	HClO ₄ (g, mmol)	Catalyst (g)	CH ₂ Cl ₂ /H ₂ O (v/v, mL)	% Conv.	% products formation			
							% Mono-bromo	% Di-bromo	% Di-ol	% Others
1	2.38, 20	2.27, 20	2.86, 20	0.010	20/20	65	28	0	33	4
2	2.38, 20	2.27, 20	2.86, 20	0.015	20/20	68	27	0	39	2
3	2.38, 20	2.27, 20	2.86, 20	0.020	20/20	70	28	0	40	2
4	1.18, 10	2.27, 20	2.86, 20	0.010	20/20	41	22	0	17	2
5	3.56, 30	2.27, 20	2.86, 20	0.010	20/20	81	27	0	51	3
6	3.56, 30	1.13, 10	2.86, 20	0.010	20/20	64	23	0	40	1
7	3.56, 30	3.39, 30	2.86, 20	0.010	20/20	91	22	0	66	3
8	3.56, 30	3.39, 30	1.43, 10	0.010	20/20	47	16	0	29	2
9	3.56, 30	3.39, 30	2.86, 30	0.010	20/20	99	16	2	77	4

**Fig. 8.** Percentage consumption of styrene and selectivity of the formation of products with time using PS-im[VO₂(pan)] (**4**) as a catalyst precursor for 2 h of reaction time under the optimized conditions specified in the text.

of 1:3 was considered as the best one for the maximum oxidative bromination of styrene. A similar effect along with an equally good conversion of styrene has also been observed using H₂SO₄ under similar conditions, while the use of acetic acid was not successful.

Details of all these conditions and the corresponding conversion of styrene along with the percent formation of the different products are summarized in Table 6. Thus, the optimized reaction conditions (entry No. 9) as concluded for the oxidative bromination of 10 mmol (1.04 g) of styrene under a bi-phasic system are: catalyst (0.010 g), KBr (3.57 g, 30 mmol), aqueous 30% H₂O₂ (3.39 g, 30 mmol), 70% HClO₄ (4.28 g, 30 mmol) and CH₂Cl₂-H₂O (40 mL, 50% v/v). The conversion of styrene and the formation of different reaction products under the optimized reaction conditions have been analyzed as a function of time and are presented in Fig. 8. It is clear from the plot that the formation of all three major products starts with the consumption of styrene. The selectivity of the formation of the diol improves continuously and reaches 78% at the end of 1 h. The selectivity of the mono bromo derivative improves to 20% slowly in the first 45 min and then decreases. The formation of the dibromo derivative starts only after 30 min and ends up at 2% in 1 h. Although no further increment was obtained after 1 h,

stirring the reaction mixture further affected the reaction products (see Fig. 8) and at the end of 2 h, the selectivity of the reaction products followed the order: 1-phenylethane-1,2-diol (85%) > 1,2-dibromo-1-phenylethane (8.5%) > 2-bromo-1-phenylethane-1-ol (0.5%). It seems that the monobromo derivative converts into 1-phenylethane-1,2-diol slowly.

The recycling ability of **4** was also tested for the oxidative bromination of styrene. The reaction mixture, after a contact time of 1 h, was filtered and the separated catalyst was washed with acetonitrile, dried and subjected to further catalytic reactions under similar conditions. No appreciable loss in the activity (see Table 7) indicated that the catalyst was active even after the first cycle.

The neat complex [(VO(pan))₂(μ-O)₂] (**2**) showed 90% conversion of styrene using 0.0007 g under the above optimized conditions. However, the turnover frequency was low compared to that of the polymer-anchored complex. The formation of only 2-bromo-1-phenylethane-1-ol and 1-phenylethane-1,2-diol was observed at the end 1 h of reaction. The 1,2-dibromo-1-phenylethane product starts forming only after 1 h, along with a small amount of an unidentified product, but the overall formation of both products are very low even after 2 h. The selectivity of the reaction products has the following order: 1-phenylethane-1,2-diol (75%) > 2-bromo-1-phenylethane-1-ol (20%) > 1,2-dibromo-1-phenylethane (1.2%). In the absence of catalyst, the reaction mixture gave about 55% conversion after 1 h of reaction time under the above optimized reaction conditions, with the selectivity order of products: 1-phenylethane-1,2-diol (58%) > 2-bromo-1-phenylethane-1-ol (35%) > others (7%) > 1,2-dibromo-1-phenylethane (0%).

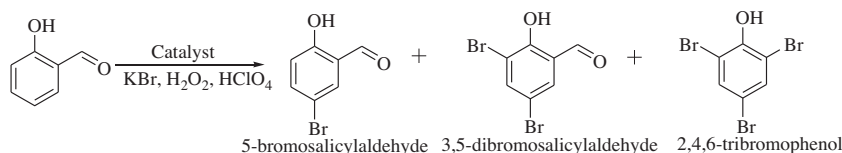
The catalytic efficiency of PS-im[VO₂(pan)] cannot be compared with similar catalytic systems as no catalytic activity for the oxidative bromination of styrene using other polymer-grafted complexes has been reported in the literature. However, the catalytic potential of PS-im[VO₂(pan)] compares well with several other mononuclear and binuclear V^V complexes [22] and even with a manganese complex [34]. The geometry and ligand environments (e.g. ONO or ONS donor) do not have much effect on the catalytic potential of the complexes and exhibit almost similar conversion along with the formation of all three products. The dioxidovanadium(V) complexes with sterically hindered ONO donor ligands gave relatively more amounts of 2-bromo-1-phenylethane-1-ol

Table 7

Conversion of styrene and the selectivity of products under the optimized reaction condition after 1 h of reaction time.

SL.No.	Catalyst	% Conv.	TOF/h ⁻¹	Selectivity (%)			
				Mono-bromo	Di-bromo	Di-ol	Others
1.	PS-im[VO ₂ (pan)]	99	4648	16	2	78	4
2.	PS-im[VO ₂ (pan)] ^a	95	4460	15	2	79	4
3.	[(VO(pan)) ₂ (μ-O) ₂]	90	4226	24	0	73	3

^a First cycle of used catalyst.



Scheme 4. Oxidative brominated products of salicylaldehyde.

Table 8

Results of the oxidative bromination of salicylaldehyde using the catalyst PS-im[VO₂(pan)] (**4**) after 2 h of reaction time.

Entry No.	KBr (g, mmol)	H ₂ O ₂ (g, mmol)	HClO ₄ (g, mmol)	Catalyst (g)	H ₂ O (mL)	% Conv.	% Mono-bromo	% Di-bromo	% Tri-bromo
1.	1.18, 10	1.13, 10	1.42, 10	0.005	20	96	80	14	0
2.	1.18, 10	1.13, 10	1.42, 10	0.010	20	99	84	12	3
3.	1.18, 10	1.13, 10	1.42, 10	0.015	20	99	84	10	5
4.	1.18, 10	0.56, 5	1.42, 10	0.005	20	46	37	8	1
5.	1.18, 10	1.69, 15	1.42, 10	0.005	20	96	78	6	12
6.	0.59, 5	1.13, 10	1.42, 10	0.005	20	53	44	7	2
7.	1.77, 15	1.13, 10	1.42, 10	0.005	20	98	83	12	3
8.	1.18, 10	1.13, 10	0.177, 5	0.005	20	78	67	11	0
9.	1.18, 10	1.13, 10	2.13, 15	0.005	20	99	85	14	0

(bromohydrin) [15]. However, in most cases 1-phenylethane-1,2-diol has been obtained in higher amounts.

3.9.2. Oxidative bromination of salicylaldehyde

The catalyst PS-im[VO₂(pan)] successfully performed the oxidative bromination of salicylaldehyde using the above mentioned reagents in water and gave three major products, 5-bromosalicylaldehyde, 3,5-dibromosalicylaldehyde and 2,4,6-tribromophenol (Scheme 4) at 40 °C. About 2 h was required to get maximum conversion. The oxidative bromination of salicylaldehyde has been reported earlier using vanadium complexes as catalysts [22] and the products mentioned above are common oxidative brominated products of salicylaldehyde. The reaction conditions were optimized for the maximum oxidative bromination considering different parameters, like amounts of catalyst, aqueous 30% H₂O₂, KBr and 70% HClO₄. Thus for 5 mmol (0.61 g) of salicylaldehyde, three different amounts of catalyst (0.005, 0.010 and 0.015 g), aqueous 30% H₂O₂ (5, 10 and 15 mmol), KBr (5, 10 and 15 mmol) and 70% HClO₄ (5, 10 and 15 mmol, added in four equal portions to the reaction mixture, first portion at $t = 0$ and the other three portions after 30 min intervals) were taken in water and the reaction was carried out. After several trials (see Table 8), the optimized reaction conditions for the maximum conversion of salicylaldehyde were obtained and these were: salicylaldehyde (0.61 g, 5 mmol), KBr (1.18 g, 10 mmol), aqueous 30% H₂O₂ (1.13 g, 10 mmol), catalyst precursor (0.005 g), aqueous 70% HClO₄ (1.42 g, 10 mmol) and water (20 mL). The conversion of salicylaldehyde under various reactions conditions and the formation of different products after 2 h of reaction time are presented in Table 8.

Table 9 compares the selectivity of the products obtained by grafted, grafted but recycled and neat catalysts. The recycled catalyst showed slightly less conversion than that obtained by a fresh one, but the selectivity of the different products are nearly the same

Table 9

Product selectivity and % conversion under the optimized reaction conditions for salicylaldehyde.

SL.No.	Catalyst (g, mmol)	% Conv.	TOF/h ⁻¹	Product selectivity (%)		
				Mono-bromo	Di-bromo	Tri-bromo
1.	PS-im[VO ₂ (pan)]	96	2254	81	6	13
2.	PS-im[VO ₂ (pan)] ^a	92	2160	80	6	14
3.	[(VO(pan)) ₂ (μ-O) ₂]	80	1878	86	14	0

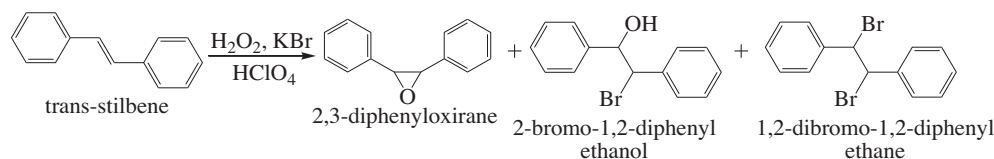
^a First cycle of used catalyst.

and follows the order: 5-bromosalicylaldehyde > 2,4,6-tribromophenol > 3,5-dibromosalicylaldehyde. The non-polymer bound catalyst exhibited 80% conversion with the formation of 5-bromosalicylaldehyde (86%) and 3,5-dibromosalicylaldehyde (14%), and thus also showed a good catalytic activity. In the absence of the catalyst, the reaction mixture gave about 60% conversion of salicylaldehyde under the above optimized reaction conditions, with 82% selectivity of the mono-bromo and 18% of the di-bromo derivative.

The catalytic efficiency of the polymer-grafted complex **4** compares well with the non-grafted vanadium complexes reported in the literature [22], but its recyclable ability and high turnover frequency makes it better over the neat complexes.

3.9.3. Oxidative bromination of *trans*-stilbene

NH₄VO₃ catalyzed oxidative bromination of *trans*-stilbene in aqueous medium in the presence of H₂O₂, KBr and HBr has been reported by Hirao et al. [35] Using dodecyltrimethylammonium bromide as a surfactant facilitated the bromination in 51% yield with two reaction products, namely 1,2-dibromo-1,2-diphenylethane and 2-bromo-1,2-diphenylethanol. We have carried out the oxidative bromination of *trans*-stilbene in a biphasic chloroform-water system. Chloroform was found to be a better solvent in terms of solubility of *trans*-stilbene and the reaction products. The oxidative bromination of *trans*-stilbene gave mainly three products: (i) 2,3-diphenyloxirane (*trans*-stilbene oxide), (ii) 2-bromo-1,2-diphenylethanol and (iii) 1,2-dibromo-1,2-diphenylethane; Scheme 5. About 2 h was required to get the maximum conversion. The reaction conditions for the maximum oxidative bromination of *trans*-stilbene were also optimized considering all the parameters mentioned above, such as amounts of catalyst, aqueous 30% H₂O₂, KBr and 70% HClO₄. Their details, the corresponding oxidative bromination of substrate under various conditions and % selectivity of different products are summarized in Table 10. It is clear



Scheme 5. Products obtained upon oxidative bromination of *trans*-stilbene.

Table 10

Results of oxidative bromination of *trans*-stilbene using the catalyst Ps-im[VO₂(pan)] after 2 h of reaction time.

Entry No.	KBr (g, mmol)	H ₂ O ₂ (g, mmol)	HClO ₄ (g, mmol)	Catalyst (g)	Solvent (mL) (CHCl ₃ /H ₂ O)	% Conv.	% Mono-bromo	% Di-bromo	% T.S.O. ^a	% Others
1	3.56, 30	3.39, 30	5.72, 40	0.005	20/20	96	4	28	62	2
2	3.56, 30	3.39, 30	5.72, 40	0.010	20/20	98	5	28	63	2
3	3.56, 30	3.39, 30	5.72, 40	0.015	20/20	99	5	29	63	2
4	1.18, 10	3.39, 30	5.72, 40	0.005	20/20	79	6	22	48	3
5	2.36, 20	3.39, 30	5.72, 40	0.005	20/20	92	3	28	58	3
6	2.36, 20	1.13, 10	5.72, 40	0.005	20/20	85	7	21	55	2
7	2.36, 20	2.27, 20	5.72, 40	0.005	20/20	91	7	22	60	2
8	2.36, 20	2.27, 20	2.86, 20	0.005	20/20	70	5	18	45	2
9	2.36, 20	2.27, 20	4.29, 30	0.005	20/20	86	6	22	56	2

^a T.S.O. = *trans*-stilbene oxide.

Table 11

Product selectivity and % conversion under the optimized reaction conditions for *trans*-styrene.

SL.No.	Catalyst	% Conv.	TOF/ h ⁻¹	Selectivity (%)			
				Mono-bromo	Di-bromo	T.S.O	Others
1.	PS-im[VO ₂ (pan)]	91	2136	8	24	66	2
2.	PS-im[VO ₂ (pan)] ^a	87	2043	11	21	65	3
3.	[[V ^{IV} O(pn)] ₂ (μ-O) ₂]	72	1690	16	20	62	2

^a First cycle of used catalyst.

from the table that the optimized reaction conditions for this reaction are different from other two reactions mentioned above and they are (entry No. 7): *trans*-stilbene (0.90 g, 5 mmol), KBr (2.36 g, 20 mmol) aqueous 30% H₂O₂ (2.27 g, 20 mmol) catalyst precursor (0.005 g), aqueous 70% HClO₄ (5.72 g, 40 mmol) and CHCl₃-H₂O (40 mL, 50% v/v). Under these conditions, a maximum of 91% conversion of *trans*-stilbene was obtained, where selectivity of the reaction products follows the order: 2,3-diphenyloxirane (*trans*-stilbene oxide) (66%) > 1,2-dibromo-1,2-diphenylethane (24%) > 2-bromo-1,2-diphenylethanol (8%).

Table 11 compares the conversion of *trans*-stilbene, obtained by the fresh and recycled grafted catalysts, and the non-polymer grafted catalyst, along with the selectivity of the products. The recycled catalyst again showed slightly less conversion (87%) than that obtained by a fresh catalyst. The non-grafted catalyst exhibits even lower conversion (72%). However, the selectivity of the formation of all three products is nearly same for all catalysts and follows the same order as mentioned above. In the absence of the catalyst, the reaction mixture gave about 55% conversion under above optimized reaction conditions with 81% selectivity of *trans*-stilbene oxide, 15% of 1,2-dibromo-1,2-diphenylethane and 2% of 2-bromo-1,2-diphenylethanol.

3.10. Reactivity of oxidovanadium(IV) and dioxidovanadium(V) complexes and possible mechanism of the oxidative bromination of substrates

The generally accepted mode of action of V-BrPOs involves the presence of vanadium in their active sites, where the V ion serves as a strong Lewis acid in the activation of the primary oxidant,

H₂O₂, and forms a peroxido vanadium derivative. In the presence of KBr and HClO₄, it oxidizes a bromide ion, giving a bromine equivalent (most likely HOBr) intermediate. Such an intermediate may then brominate an appropriate organic substrate. The possibility of involving an intermediate containing vanadium bound OBr⁻, in the presence of H₂O₂, KBr and HClO₄, has recently been exploited through DFT calculations [15]. The processes occurring in the aqueous phase require acidic conditions, probably to promote the protonation of the peroxido moiety.

We have monitored the reactivity of [V^{IV}O(acac)(pan)] (**1**) with H₂O₂ in DMSO by electronic absorption spectroscopy. Thus, the stepwise addition of one drop portions of 30% H₂O₂ (0.058 g, 0.513 mmol) in 10 ml of DMSO to 10 ml of ca. 10⁻⁴ M solution of **1** in DMSO results in the flattening of the shoulder band appearing at ca. 745 nm (Fig. 9 (a)). In dilute solution (ca. 10⁻⁴ M) of complex, the intensity of the 540 and 567 nm bands decreases with a slight red shift towards 552 and 581 nm, while the 502 and 411 nm bands shift to 471 and 441 nm, respectively, with a slight increase in intensity; Fig. 9(b). In the UV region, the intensity of the weak shoulder at ca. 298 nm decreases and a new shoulder band at 307 nm is generated (same as in the peroxo complex). The intensity of the band around 257 nm slowly decreases. The shape of the final spectrum is almost the same as the one obtained after treating **2** with H₂O₂, which, in turn, is similar to the spectrum of the peroxide complex **3**, thus verifying the formation of similar oxidoperoxido species with both complexes.

We have also recorded the spectral changes during stepwise additions of two drop portions of 30% H₂O₂ in 5 ml of MeOH to 25 ml of a 0.51 × 10⁻⁴ M solution of **2** in CHCl₃ (see Fig. S1 of supporting information). The spectral changes observed are very sim-

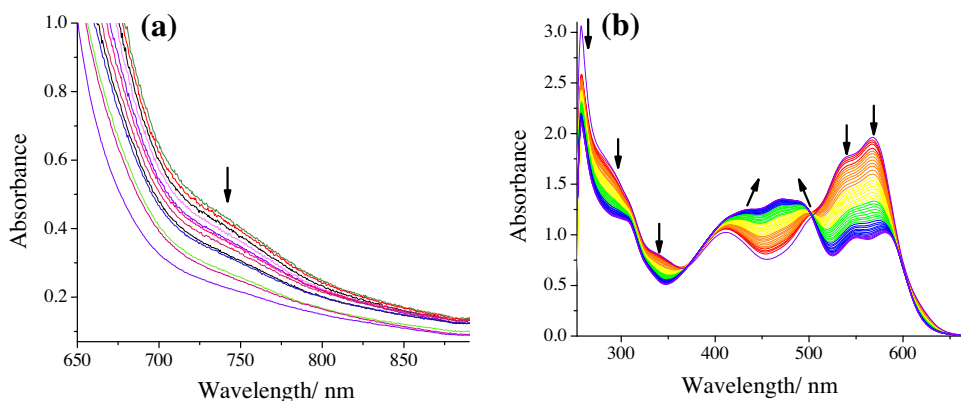


Fig. 9. Spectral changes obtained during titration of (a) stepwise addition of one drop portions of 30% H_2O_2 (0.058 g, 0.513 mmol) in 10 ml of DMSO to 10 ml of ca. 10^{-4} M solution of $[\text{V}^{\text{IV}}\text{O}(\text{acac})(\text{pan})]$ (**1**) in DMSO and (b) stepwise additions of one drop portions of aqueous 30% (0.058 g, 0.513 mmol) in 5 ml of DMSO to 20 ml of ca. 1.58×10^{-4} M solution of **1** in DMSO.

ilar to the ones recorded in DMSO, showing the formation of similar types of species in both solutions.

Upon addition of 1.0 equiv. of a 30% aqueous H_2O_2 to a methanolic solution of **2** (ca. 4 mM), a peak at $\delta = -597$ ppm emerges, which we assigned to $[\text{V}^{\text{V}}\text{O}(\text{O}_2)\text{ONN}(\text{S})]$ ($\text{S} = \text{solvent}$). This signal increases in intensity at the expense of the resonances due to the dioxido species ($\delta = -542$ ppm) upon further addition of H_2O_2 . The signals due to the dioxido species finally disappear and another weak signal at $\delta = -644$ ppm, in addition to the signal due to the peroxido complex, also builds up upon addition of a total of 4 equiv. of H_2O_2 , which is possibly due to $[\text{V}^{\text{V}}\text{O}(\text{O}_2)_2\text{S}]$ (Fig. 10) [36]. Leaving the NMR tube open for 24 h, the only resonance at -549 ppm due to **2**-MeOD is recorded, indicating the reversibility of the process [37].

In order to identify the possible intermediate forms in the catalytic reaction, the reactivity of the peroxido complex $[\text{V}^{\text{V}}\text{O}(\text{O}_2)(\text{pan})(\text{MeOH})]$ (**3**) in methanol with one drop portions of saturated HCl solution in 5 ml of MeOH has also been studied and the spectral changes are presented in Fig. 11. The bands at 420 and 490 nm in the visible region are mainly affected in the presence of HCl. Thus the band at 420 shifts to 410 nm with an increase in intensity,

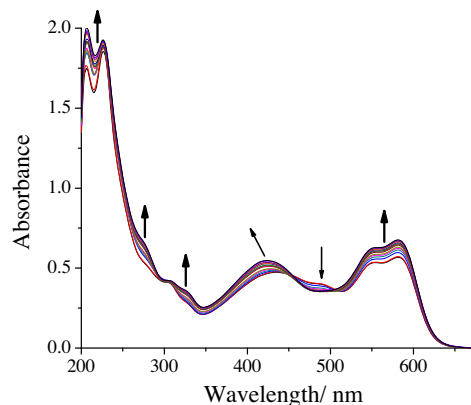


Fig. 11. Spectral changes obtained during the titration of stepwise additions of one drop portions of saturated HCl in 5 ml of MeOH to 25 ml of ca. 2.03×10^{-4} M solution of $[\text{V}^{\text{V}}\text{O}(\text{O}_2)(\text{pan})(\text{MeOH})]$ (**3**) in MeOH.

while the 490 nm band completely disappears. Other bands at 550 and 590 nm gain only in intensity, without changing their positions. These spectral changes have been proposed to be due to the formation of oxidohydroperoxido species [15,38–41].

Thus, the complexes reported here show similar behaviour as shown by other model complexes. As observed in other model vanadium complexes [11,33,42], in the presence of KBr, H_2O_2 and HClO_4 , the generated HOBr during the catalytic reaction may react with styrene to give the bromonium ion as an intermediate. The nucleophile Br^- as well as H_2O both may attack the α -carbon of the intermediate to give 1,2-dibromo-1-phenylethane and 2-bromo-1-phenylethane-1-ol, respectively (Scheme 6). The formation of the dibromo product in most cases at a later stage is possibly due to (i) the presence of a lesser amount of brominating reagent generated initially and/or (ii) the generation of a lesser amount of Br_2 , another intermediate, during the catalytic action. The nucleophile H_2O may further attack the α -carbon of 2-bromo-1-phenylethane-1-ol to give 1-phenylethane-1,2-diol. All these justify the formation of 1-phenylethane-1,2-diol in higher yield.

The formation of 5-bromosalicylaldehyde and 3,5-dibromosalicylaldehyde upon oxidative bromination of salicylaldehyde is expected as the $-\text{OH}$ group of salicylaldehyde is *ortho* and *para* directing. However, the formation of 2,4,6-tribromophenol is possible only through decarbonylative bromination. Rana et al. [43] have recently shown that a vanadium bound OCl^- species interacts with a substrate like 2-hydroxy-1-naphthaldehyde using both

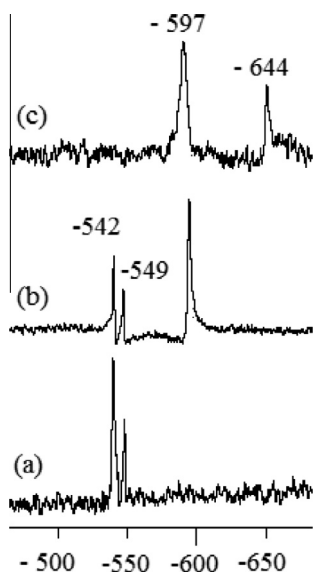
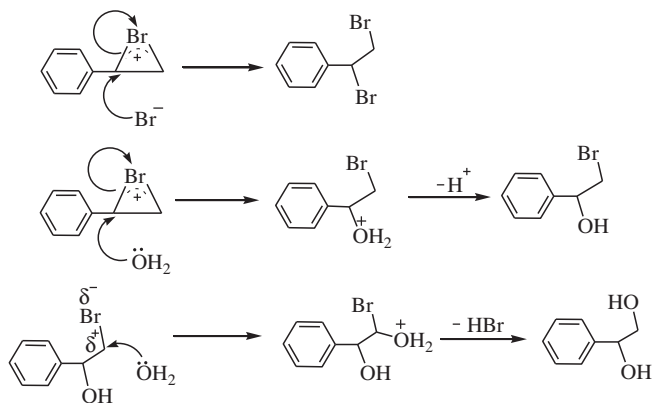


Fig. 10. ^{51}V NMR spectra of methanolic solutions of complex **3** (ca. 4 mM): (a) after preparation of the solution, (b) solution of (a) after addition of 1 equiv. H_2O_2 , (c) solution of (a) after 1 h of addition of 4 equiv. H_2O_2 .



Scheme 6. Mechanism of action of HOBr on styrene.

functional groups, which in the presence of H_2O_2 and KCl provides the decarbonylated chlorinated product 1-chloronaphthalen-2-ol. Such a mechanism is partly applicable here as well to give 2-bromophenol from salicylaldehyde, which may undergo further bromination to give 2,4,6-tribromophenol.

The formation of 1,2-dibromo-1,2-diphenylethane and 2-bromo-1,2-diphenylethane by oxidative bromination of *trans*-stilbene is again possible through a bromonium ion intermediate, as mentioned above for the oxidative bromination of styrene, while that of 2,3-diphenyloxirane (*trans*-stilbene oxide) is the expected product by regular oxidation of *trans*-stilbene.

3.11. Leaching study of vanadium from the polymer-anchored catalyst

To find out whether the acid (HClO_4) added really causes leaching of the vanadium ion (i.e. inorganic vanadium), we have performed a blank reaction under the optimized reaction conditions, e.g. for oxidative bromination of *trans*-stilbene [i.e. catalyst precursor (0.005 g), KBr (2.36 g, 20 mmol), aqueous 30% H_2O_2 (2.27 g, 20 mmol), 70% HClO_4 (5.72 g, 40 mmol, added in four equal portions at 15 min intervals) and CHCl_3 - H_2O (40 mL, 50% v/v)] but without substrate and tested the aqueous layer after 1 h by electronic absorption spectroscopy. While the aqueous layer from the experiment does not show any band at ca. 400 nm, the standard solution made by dissolving V_2O_5 in H_2O_2 shows a detectable band at ca. 400 nm; Fig. S2. As H^+ ions are consumed continuously in the formation of possibly hydroperoxide intermediate species during the catalytic reaction, the added perchloric acid is consumed continuously and thus avoids the decomposition of the catalysts. However, the aqueous layer from the blank reaction showed a vanadium content of 0.02 mmol g^{-1} of resin, which indicates only partial leaching of the complex from the polymer beads. An equally good catalytic activity of the recycled catalyst further supports only partial decomposition of the polymer-anchored complex during the catalytic reactions.

4. Conclusions

The monobasic tridentate ONN donor ligand 1-(2-pyridylazo)-2-naphthol [Hpan (**1**)] has been used to prepare the oxidovanadium(IV) complex $[\text{V}^{\text{IV}}\text{O}(\text{acac})(\text{pan})]$ (**1**). Areal oxidation of **1** gave the dioxidovanadium(V) complex $[\{\text{V}^{\text{V}}\text{O}(\text{pan})\}_2(\mu\text{-O})_2]$ (**2**), which can be considered to be a structural model of haloperoxidase. Complex **2** has been grafted successfully through covalent bonding with imidazole appended methylpolystyrene cross-linked with 5% divinylbenzene [now abbreviated as PS-im $[\text{V}^{\text{V}}\text{O}_2(\text{pan})]$ (**4**)]. Oxidative bromination of styrene, salicylaldehyde and *trans*-

stilbene has been successfully carried out using **4** as a heterogeneous catalyst, demonstrating the functional similarity to haloperoxidases. The recyclable ability and better catalytic ability over the non-grafted analog make it useful functional model of haloperoxidases. A peroxide species similar to $[\text{V}^{\text{V}}\text{O}(\text{O}_2)(\text{pan})](\text{MeOH})$ (**3**), that has been isolated in the solid state, has also been demonstrated to form in solution, which on reaction with acid possibly generates a hydroperoxide intermediate during the catalytic action. Possible mechanisms for the formation of different reaction products upon oxidative bromination of the above substrates have been proposed.

Acknowledgments

The authors thank the Council of Scientific and Industrial Research (CSIR), New Delhi (India) for research project No. 01/(2447)/10-EMR-II and the Department of Science and Technology, New Delhi (India) for research project No. SR/S1/IC-32/2010. The authors are also thankful to Prof. J. Costa Pessoa for recording the EPR and ^{51}V NMR spectra that appear in this paper. NC thanks CSIR for the award of a Junior Research Fellowship.

Appendix A. Supplementary data

CCDC 941405 contains the supplementary crystallographic data for **3**. These data can be obtained free of charge via <http://www.ccdc.cam.ac.uk/conts/retrieving.html>, or from the Cambridge Crystallographic Data Centre, 12 Union Road, Cambridge CB2 1EZ, UK; fax: +44 1223 336 033; or e-mail: deposit@ccdc.cam.ac.uk. Supplementary data associated with this article can be found, in the online version, at <http://dx.doi.org/10.1016/j.poly.2013.09.021>.

References

- [1] A. Messerschmidt, R. Wever, Proc. Natl. Acad. Sci. USA 93 (1996) 392.
- [2] M. Weyand, H.J. Hecht, M. Kiesz, M.F. Liaud, H. Vilter, D. Schomburg, J. Mol. Biol. 293 (1999) 595.
- [3] M.I. Isupov, A.R. Dalby, A. Brindley, Y. Izumi, T. Tanabe, G.N. Murshudov, J.A. Littlechild, J. Mol. Biol. 299 (2000) 1035.
- [4] D. Rehder, Bioinorganic Vanadium Chemistry, John Wiley & Sons, Chichester, 2008.
- [5] A.G.J. Ligtenberg, R. Hage, B.L. Feringa, Coord. Chem. Rev. 237 (2003) 89.
- [6] V. Conte, A. Coletti, B. Floris, G. Licini, C. Zonta, Coord. Chem. Rev. 255 (2011) 2165.
- [7] J.A.L. da Silva, J.J.R. Fraústo da Silva, A.J.L. Pombeiro, Coord. Chem. Rev. 255 (2011) 2232.
- [8] M.R. Maurya, A. Kumar, J. Costa Pessoa, Coord. Chem. Rev. 255 (2011) 2315.
- [9] M.R. Maurya, J. Costa Pessoa, J. Organomet. Chem. 696 (2011) 244.
- [10] M.R. Maurya, J. Chem. Sci. 123 (2011) 215.
- [11] P. Adão, J. Costa Pessoa, R.T. Henriques, M.L. Kuznetsov, F. Avecilla, M.R. Maurya, U. Kumar, I. Correia, Inorg. Chem. 48 (2009) 3542.
- [12] M.R. Maurya, Coord. Chem. Rev. 237 (2003) 163.
- [13] A. Mondal, S. Sarkar, D. Chopra, T.N.G. Row, K. Pramanik, K.K. Rajak, Inorg. Chem. 44 (2005) 703.
- [14] M.R. Maurya, S. Agarwal, C. Bader, D. Rehder, Eur. J. Inorg. Chem. (2005) 147.
- [15] M.R. Maurya, C. Haldar, A. Kumar, M.L. Kuznetsov, F. Avecilla, J. Costa Pessoa, Dalton Trans. 42 (2013), <http://dx.doi.org/10.1039/c3dt50469g>.
- [16] M.R. Maurya, M. Kumar, A. Arya, Catal. Commun. 10 (2008) 187.
- [17] G. Grivani, S. Tangestaninejad, M.H. Habibi, V. Mirkhani, M. Moghadam, Appl. Catal. A: Gen. 299 (2006) 131.
- [18] R.A. Rowe, M.M. Jones, Inorg. Synth. 5 (1957) 113.
- [19] A. Rockenbauer, L. Korecz, Appl. Magn. Reson. 10 (1996) 29.
- [20] M.R. Maurya, P. Saini, C. Haldar, F. Avecilla, Polyhedron 31 (2012) 710.
- [21] G.M. Sheldrick, SHELXL-97: An Integrated System for Solving and Refining Crystal Structures from Diffraction Data (Revision 5.1), University of Göttingen, Germany, 1997.
- [22] M.R. Maurya, C. Haldar, A.A. Khan, A. Azam, A. Salahuddin, A. Kumar, J. Costa Pessoa, Eur. J. Inorg. Chem. (2012) 2560.
- [23] H. Kelm, H.-J. Krüger, Angew. Chem. Int. Ed. 40 (2001) 2344.
- [24] M. Kaliva, C. Gabriel, C.P. Raptopoulou, A. Terzis, G. Voyiatzis, M. Zervou, C. Mateescu, A. Salifoglou, Inorg. Chem. 50 (2011) 11423.
- [25] C.R. Waidmann, A.G. DiPasquale, J.M. Mayer, Inorg. Chem. 49 (2010) 2383.
- [26] S. Basu, S. Halder, I. Pal, S. Samanta, P. Karmakar, M.G.B. Drew, S. Bhattacharya, Polyhedron 27 (2008) 2943.
- [27] (a) M.R. Maurya, S. Khurana, W. Zhang, D. Rehder, J. Chem. Soc., Dalton Trans. (2002) 3015.

- [28] M.R. Maurya, A. Arya, A. Kumar, M.L. Kuznetsov, F. Avecilla, J. Costa Pessoa, *Inorg. Chem.* 49 (2010) 6586.
- [29] K. Wüthrich, *Helv. Chim. Acta* 48 (1965) 1012.
- [30] N.D. Chasteen, in: J. Reuben (Ed.), *Biological Magnetic Resonance*, Plenum, New York, 1981, p. 53.
- [31] E. Garriba, G. Micera, D. Sanna, *Inorg. Chim. Acta* 359 (2006) 4470.
- [32] D. Rehder, C. Weidemann, A. Duch, W. Pribsch, *Inorg. Chem.* 27 (1988) 584.
- [33] A. Butler, in: J. Reedijk, E. Bouwman (Eds.), *Bioinorganic Catalysis*, 2nd ed., Marcel Dekker, New York, 1999, p. 55 (Chapter 5).
- [34] V. Conte, B. Floris, *Inorg. Chim. Acta* 363 (2010) 1935.
- [35] M.R. Maurya, P. Saini, C. Haldar, F. Avecilla, *Polyhedron* 46 (2012) 33.
- [36] T. Moriuchi, M. Yamaguchi, K. Kikushima, Hiraio, *Tetrahedron Lett.* 48 (2007) 2667.
- [37] M.R. Maurya, P. Saini, A. Kumar, J. Costa Pessoa, *Eur. J. Inorg. Chem.* (2011) 4846.
- [38] V. Conte, F.D. Furla, S. Moro, *J. Mol. Catal. A: Chem.* 104 (1995) 159.
- [39] G.J. Colpas, B.J. Hamstra, J.W. Kampf, V.L. Pecoraro, *J. Am. Chem. Soc.* 118 (1996) 3469.
- [40] M.R. Maurya, A.A. Khan, A. Azam, S. Ranjan, N. Mondal, A. Kumar, J. Costa Pessoa, *Eur. J. Inorg. Chem.* (2009) 5377.
- [41] M.R. Maurya, A.A. Khan, A. Azam, S. Ranjan, N. Mondal, A. Kumar, F. Avecilla, *J. Costa Pessoa, Dalton Trans.* 39 (2010) 1345.
- [42] C.J. Schneider, J.E. Penner-Hahn, V.L. Pecoraro, *J. Am. Chem. Soc.* 130 (2008) 2712.
- [43] S. Rana, R. Haque, G. Santosh, D. Maiti, *Inorg. Chem.* 52 (2013) 2927.